EXTENDED EXPERIMENTAL PROCEDURES

Mice

C57BL/6, CD45.1 (inbred C57BL/6), Balb/c and CB6F1 mice were purchased from Charles River. Thy1.1 (CBy.PL(B6)-*Thy1*^{a}/ScrJ), CD44$^{-/-}$ (B6.129(Cg)-Cd44tm1Hbg/J), P-selectin$^{-/-}$ (B6.129S7-*Selp*^{tm1Bay}/J), ROSA$^{mT/mG}$ (B6.129(Cg)-*Gt(ROSA)26Sor*$^{tm4(ACTB-tdTomato,-EGFP)Luo}$/J), Alb-cre mice (B6.Cg-Tg(Alb-cre)21Mgn/J) and β-actin-GFP (C57BL/6-Tg(CAG-EGFP)1Osb/J) mice were purchased from The Jackson Laboratory. CD40L$^{-/-}$ (B6.129S2-*Cd40*^{tm1Imx}/J) and P14 (B6-Tg(TCRP14)327Zbz-Ly5.1) mice were obtained through the Swiss Immunological Mutant Mouse Repository (Zurich, Switzerland). Mice genetically deficient for mouse GP-Ibα and transgenic for human GP-Ibα (mGP-Ibα^{null};hGP-Ibα^{Tg}) have been previously described (Ware et al., 2000). Mice lacking tryptophan hydroxylase (TPH) 1 (inbred C57BL/6) were provided by Michael Bader (Max-Delbrück-Center for Molecular Medicine). HBV replication-competent transgenic mice (lineage 1.3.32, inbred C57BL/6, H-2^{b}), that express all of the HBV antigens and replicate HBV in the liver at high levels without any evidence of cytopathology, have been previously described (Guidotti et al., 1995). In indicated experiments, these mice were bred for > 10 generations against Balb/c mice or used as C57BL/6 x Balb/c H-2^{bxd} F1 hybrids. HBcAg transgenic mice (lineage MUP-core 50 [MC50], inbred C57BL/6, H-2^{b}), that express the HBV core protein in 100% of the hepatocytes under the transcriptional control of the mouse major urinary protein (MUP) promoter, have been previously described (Guidotti et al., 1994). In indicated experiments, HBcAg transgenic mice were bred against Alb-cre x ROSA$^{mT/mG}$ mice to generate HBcAg^{+} mice whose LSEC express membrane-targeted tdTomato and whose hepatocytes express membrane-targeted eGFP. Cor93 TCR transgenic mice (lineage BC10.3, inbred CD45.1), in which > 98% of the splenic CD8+ T cells recognize a K^{b}-restricted epitope located between residues 93–100 in the HBV core protein (MGLKFRQL), have been previously described (Isogawa et al., 2013). Env28 TCR transgenic mice (lineage 6C2.36, inbred Balb/c), in which ~83% of the splenic CD8+ T cells recognize a L^{d}-restricted epitope located between residues 28–39 of HBsAg (IPQSLDSWWTSL), have been previously described (Isogawa et al., 2013). They were mated once with Thy1.1 mice (inbred Balb/c) so that the TCR transgenic T cells could be easily followed upon adoptive transfer by anti-Thy1.1 antibody (Ab) staining.

Bone marrow chimeras were generated by irradiation of C57BL/6 mice with 1,300 rad in split doses and reconstitution with β-actin-GFP bone marrow; mice were allowed to reconstitute for at least 8 weeks prior to use. Mice were housed under specific pathogen-free conditions and used at 8-10 weeks of age, unless otherwise indicated. In all experiments, mice were matched for age, sex and (for the 1.3.32 animals) serum HBeAg levels before experimental manipulations. All experimental animal procedures were approved by the Institutional Animal Committee of the San Raffaele Scientific Institute.

Viruses and Vectors

Adenoviral vectors containing a 1.3-fold over length HBV genome and cytomegalovirus promoter-driven GFP (Ad-HBV-GFP) gene have been previously described (Sprinzl et al., 2001). Naive WT mice were injected with 2.5 × 10^{8} infectious units of Ad-HBV-GFP i.v. 2 days prior to further experimental manipulation. Adenoviral vectors expressing β-gal under the control of a truncated human cytomegalovirus promoter (Ad-β-gal) have been previously described (Iannacone et al., 2005). Mice were immunized intramuscularly with 50 μg of a plasmid that expresses the β-gal coding sequence under the control of the human CMV enhancer/promoter (pCMV-β-gal) as described (Iannacone et al., 2005) 3 weeks prior to receiving 3 × 10^{9} pfu of Ad-β-gal i.v.

LCMV Armstrong was grown and titrated as described (Iannacone et al., 2008). Mice were infected i.v. with 2 × 10^{6} focus-forming units of LCMV Armstrong 2 days prior to the injection of effector P14 T cells. For construction of adeno-associated viruses (AAV) expressing GFP and HBV core antigen (AAV-HBcAg-GFP) or HBV surface antigen (AAV-HBsAg-GFP) under the control of a liver-specific promoter (Kramer et al., 2003), HBV antigens were amplified by PCR using pSP65 HBV 1.3 as template and the following primers: CoreSalI: 5′ TTTTTTGTCGACCACCATGCAACTTTTTCACCTCTGCCTAATC 3′; Core*Sac*II: 5′ AAAAAACCGCGGCTAA CATTGAGATTCCCGAGATTGAG 3′ and Slarge*Sal*I 5′ TTTTTTGTCGACCACCATGGGGCAGAATCTTTCCACCAGCAATCC 3′; 3pSlarge*Sac*II 5′ AAAAAACCGCGGTTAAATGTATACCCAAAGACAAAAGAAAATTGG 3′. In both cases the forward primer contains a SalI restriction site and the reverse primer a *Sac*II restriction site. After amplification and digestion with SalI and *Sac*II, HBcAg and HBsAg sequences were cloned into a plasmid carrying the IRES-eGFP sequence (Clontech Laboratories). By digesting these plasmids with SalI and *Not*I we obtained the HBcAg-IRES-eGFP and HBsAg-IRES-eGFP sequences that were cloned into a plasmid containing the AAV inverted terminal repeats (ITRs) sequences downstream of the liver-specific alpha-1 antitrypsin promoter and upstream of a poly A sequence. Plasmids were sequenced and the expression of HBV antigens and GFP tested in vitro in HuH7 lipofectamine-transfected cells (data not shown). AAV vectors were produced, purified, and titrated as described (Vanrell et al., 2011). Naive WT mice were injected with 3 × 10^{10} pfu of either AAV-HBcAg-GFP or AAV-HBsAg-GFP 18 days prior to further experimental manipulation. All infectious work was performed in designated BSL-2 or BSL-3 workspaces, in accordance with institutional guidelines.

Generation of Effector CD8^{+} T Cells and Adoptive Transfer

In vitro generation of CD8^{+} T cells (CD8 T$_{E}$) was performed basically as described (Manjunath et al., 2001). Briefly, splenocytes from Env28, Cor93 or P14 TCR transgenic mice were incubated with 10 μg/ml of Env28-39 (L^{d}; IPQSLDSWWTSL), Cor93-100 (K^{b}; MGLKFRQL) or GP33-41 (D^{b}; KAVYNFATM) peptides (Primm), respectively, at 37°C for 1 hr, washed, and cultured in complete RPMI 1640 (10% FBS, 2 mM L-glutamine, 50 μM 2-mercaptoethanol, HEPES 10 mM, non essential amino acid 100 μM and penicillin

plus streptomycin). Two days later cells were cultured in fresh medium supplemented with 20 ng/ml of recombinant IL-2 (R&D) or with 2.5% EL-4 supernatant. Media supplemented with cytokines were replaced every 2 days. After 8 or 9 days of culture, cells were tested for the expression of CD8, CD69, CD25, CD44, CD62L, CCR7, IFN-γ and granzyme B by FACS prior to subsequent use. 10^7 cells of each cell type were injected i.v. into recipient animals. In imaging experiments, CD8 T_E were labeled with 2.5 μM CMFDA, 2.5 μM CFSE, 7.5 μM CMTPX, 10 μM CMTMR or 2.5 μM BODIPY 630/650-X (Life Technologies) for 20 min at 37°C in plain RPMI prior to adoptive transfer. Notably, virtually identical liver diseases (monitored both histologically and biochemically) were observed in HBV replication-competent transgenic mice that received either fluorescently labeled or unlabeled HBV-specific CD8 T_E (data not shown). In indicated experiments CD8 T_E were generated in vivo by infecting C57BL/6 mice with 10^6 pfu of LCMV Arm i.v. 8 days prior to splenocyte recovering. GP33-specific CD8 T_E were identified both prior to and after adoptive transfer as $CD8^+$ $CD44^{high}$ cells that produce IFN-γ upon stimulation with GP33-41 peptide. Each recipient mouse received an injection of splenocytes containing 5 × 10^6 GP33-specific CD8 T_E.

In indicated experiments, naive $CD8^+$ T cells from LNs and spleens of Cor93 TCR transgenic mice were purified by negative immunomagnetic sorting (Miltenyi Biotec).

Blocking Abs and Hyaluronidase Treatment

To investigate the role of homing molecules in the hepatic recruitment of CD8 T_E, the following blocking Abs were injected i.v. 2 hr prior to T cell transfer: anti-PSGL-1 (clone 4RA10; BioXCell; 200 μg/mouse), anti-CD62L (clone MEL-14; BioXCell; 100 μg/mouse), anti-CD62E (clone 10E9.6; BD PharMingen; 100 μg/mouse), anti-VLA-4 (clone PS/2; BioXCell; 100 μg/mouse), anti-LFA-1 (clone M17/4; BioXCell; 100 μg/mouse and clone GAME46; BD PharMingen; 25 μg/mouse), anti-PECAM-1 (clone MEC13.3; BioLegend; 100 μg/mouse), anti-VAP-1 (80 μg of clone 7-88 + 80 μg of clone 7-106/mouse, both provided by S. Jalkanen), anti-CD44 (clone KM81, blocking CD44 binding to hyaluronan (Zheng et al., 1995); Cedarlane; 20 μg/mouse), anti-CD44 (clone IM7, not interfering with CD44 binding to hyaluronan (Zheng et al., 1995); BioXCell; 100 μg/mouse). In indicated experiments mice were injected i.p. with 20 U/g hyaluronidase type-IV (Sigma-Aldrich), a procedure that was previously determined to deplete hyaluronic acid from the vascular endothelium (Johnsson et al., 1999).

Env28 CD8 T_E-Mediated Induction of Liver Inflammation

In order to increase the hepatic expression of selectins, integrin ligands and chemokines (experiments described in Figures 2F, 2G, and S1), HBV replication-competent transgenic mice were injected i.v. with 5 × 10^6 Env28 CD8 T_E 24 hr prior to the injection of 10^7 Cor93 CD8 T_E.

Treatment with Pertussis Toxin and Chemotaxis Assay

The role of Gαi signaling was assessed by incubating CD8 T_E (10^7 cells/ml) for 2 hr at 37°C with 100 ng/ml pertussis toxin (Merck). Chemotaxis assays were performed in 24-well plates with 5 μm pore filters (Costar). 5 × 10^5 PTX-treated or control CD8 T_E were loaded in the upper chamber. The lower chamber contained media with or without the indicated concentrations of CCL2 or CXCL10 (both from R&D Systems). After 90 min at 37°C, cells in the bottom well were counted. The chemotactic index was calculated as the ratio of cells that migrated to CCL2 or CXCL10 versus cells that migrated to media alone.

Depletion, Transfusion, and Aggregation of Platelets

HBV replication-competent x mGP-Ibα^{null};hGP-Ibα^{Tg} mice were injected i.v. with 80 μg of clone LJ-P3 (a monoclonal Ab that recognizes the platelet-specific human GP-Ibα) at least 3 hr prior to further experimental manipulation. As previously described (Iannacone et al., 2008), and herein confirmed by the use of an automated cell counter (HeCoVet; Seac–Radim), this treatment selectively depletes ~98% of circulating platelets within few minutes of a single LJ-P3 Ab injection, and this thrombocytopenic state is maintained for at least 3-4 days (data not shown). Platelet transfusion was performed as described (Iannacone et al., 2008). Each mouse received a single i.v. injection of 6 × 10^8 platelets from WT, P-selectin$^{-/-}$, CD40L$^{-/-}$, CD44$^{-/-}$ or β-actin-GFP mice. Platelet aggregation in the presence of 5 μM ADP (Mascia Brunelli), 4 μg/ml fibrillar type I collagen (Mascia Brunelli) or 75 μM arachidonic acid (Mascia Brunelli) was performed as described (Iannacone et al., 2008).

Treatment with Sodium Arsenite or Carbon Tetrachloride

In indicated experiments mice were treated with sodium arsenite (250 ppb in drinking water ad libitum) for 10 weeks. In other experiments mice were fed by oral gavage with a solution of carbon tetrachloride (CCl_4) in peanut oil (Sigma–Aldrich) at a final dose of 0.7 mg/g of body weight. CCl_4 was administered twice a week for 12 weeks, after which the treatment was suspended for a washout period of 4 weeks.

Cell Isolation and Flow Cytometry

Single-cell suspensions of livers, spleens, and lymph nodes were generated as described (Iannacone et al., 2005; Tonti et al., 2013). For analysis of ex-vivo intracellular cytokine production, cell suspensions of livers were obtained as described above except that 1 μg/ml of brefeldin A (Sigma) was included in the digest buffer. All flow cytometry stainings of surface-expressed and intracellular molecules were performed as described (Tonti et al., 2013). Abs used included PB-, Alexa Fluor 488- and Alexa Fluor 647-conjugated

anti-CD8α (53-6.7), Alexa Fluor 488-, PE-, PerCP-, Alexa Fluor 647 and APC-Cy7-conjugated anti-CD45.1 (A20), Alexa Fluor 488-, PE-, PerCP-, Alexa Fluor 647- and APC-Cy7-conjugated anti-Thy1.1 (OX-7), Alexa Fluor 488-, PE- and Alexa Fluor 647-conjugated anti-IFN-γ (XMG1.2), Alexa Fluor 488-conjugated anti-CD69 (H1.2F3), PE-conjugated anti-CD25 (PC61), Alexa Fluor 488- and PE-Cy7-conjugated anti-CD62L (Mel-14), PE-conjugated anti-CCR7 (4B12), PerCP- and APC-Cy7-conjugated anti-CD44 (IM7), APC-conjugated anti-granzyme B (GB12, Invitrogen), Alexa Fluor 488-conjugated anti-CD11a (2D7), PE-conjugated anti-CD49d (9C10 [MFR4.B]), PE-conjugated anti-PSGL-1 (2PH1, BD PharMingen), PE-conjugated anti-CD51 (RMV-7), Alexa Fluor 647-conjugated anti-PECAM-1 (MEC13.3), Alexa Fluor 488-conjugated anti-CD11b (M1/70), Alexa Fluor 647-conjugated anti-Gr-1 (RB6-8C5), PE-conjugated anti-CXCR3 (CXCR3-173). All Abs were purchased from BioLegend, unless otherwise indicated. Recombinant dimeric H-2Ld:Ig and H-2Kb:Ig fusion proteins (BD PharMingen) complexed with peptides derived from HBsAg (Env28-39), from HBcAg (Cor93-100) or from β-gal (β-gal96-103), were prepared according to the manufacturer's instructions. Dimer staining was performed exactly as described (Iannacone et al., 2005). All flow cytometry analyses were performed in FACS buffer containing PBS with 2 mM EDTA and 2% FBS on a FACS CANTO (BD PharMingen) and analyzed with FlowJo software (Treestar).

Isolation of Primary Hepatocytes, Liver Sinusoidal Endothelial Cells, Kupffer Cells, Intrahepatic Dendritic Cells, and Dendritic Cells from Liver-Draining Lymph Nodes

Primary hepatocytes, liver sinusoidal endothelial cells (LSEC), Kupffer cells and dendritic cells were isolated essentially as described (Isogawa et al., 2013) from the liver of unmanipulated HBV replication-competent and HBcAg transgenic mice. Briefly, livers were perfused via the inferior vena cava with 25 ml of warm Liver Perfusion Medium (Invitrogen) at a rate of 5 ml/min, and then digested with 50–75 ml of warm Liver Digest Medium (Invitrogen) at a rate of 5 ml/min. Following complete digestion of the liver (10–15 min), the gallbladder was removed and the liver carefully excised. Cells were collected from the liver by disrupting the liver capsule and swirling the tissue in a petri dish containing Hepatocyte Wash Medium. Liver non-parenchymal cells (LNPC) containing LSEC were separated from hepatocytes by centrifuging the cell suspension at 50*g* for 3 min at room temperature. For LSEC isolation, the supernatant containing LNPC was washed twice and cells were further separated by a 36% Percoll density gradient. The cell pellet was resuspended with BD IMag Buffer at a concentration of 1×10^7/ml. The cell suspension was incubated with biotinylated anti-LYVE-1 Ab (eBioscience) (2,5 μg for every 1×10^7 of LNPC) for 15 min on ice, washed twice, and resuspended in IMag buffer at a concentration of 2×10^7 cells ml. The cell suspension was then incubated with BD IMag Streptavidin Particles Plus-DM (BD Bioscience) (20 μl for every 1×10^7 of LNPC) for 30 min on ice, washed twice, and resuspended in IMag buffer at a concentration of 2-8 $\times 10^7$ cells/ml. LYVE-1^+ cells were then positively selected using BD IMagnet (BD Bioscience) according to the manufacturer instruction. LSEC purity (assessed by flow cytometry-based positive and negative signals for CD146 and CD45, respectively) and viability (assessed by light microscopy-based morphology and Trypan blue dye exclusion) were routinely greater than 85% and 90%, respectively. For hepatocyte isolation, the pellet from the initial centrifugation step was further separated by a 36% Percoll density gradient. Hepatocyte purity (assessed by flow cytometry-based parameters of size) and viability (assessed by light microscopy-based morphology and Trypan blue dye exclusion) were routinely greater than 70% and 80%, respectively. The isolation of Kupffer cells was performed by selective adherence, as described (Smedsrød and Pertoft, 1985). Briefly, the supernatant containing LNPC was seeded in 6 well plates and allowed to adhere for 3 hr at 37°C before the medium containing non-adherent cells was removed. Kupffer cell purity (assessed by flow cytometry-based positive signals for CD11b and F4/80) and viability (assessed by light microscopy-based morphology and Trypan blue dye exclusion) were routinely greater than 55% and 95%, respectively. Hepatic dendritic cells were isolated by positive selection using biotinylated CD11c and streptavidin Magnetic Particles (BD Biosciences), as previously described (Isogawa et al., 2013). Hepatic DC purity, assessed by CD11c staining, was routinely greater than 80% and viability higher than 95%. Hepatic lymph node dendritic cells were isolated by positive selection using biotinylated CD11c and streptavidin Magnetic Particles (BD Biosciences). Lymph node DC purity, assessed by CD11c staining was routinely greater than 90% and viability higher than 95%. Hepatocytes, LSEC, Kupffer cells or DCs (10^6 cells/ml) were incubated at a 1:1 ratio with Cor93 or Env28 CD8 T_E for 4 hr in the presence of 10 μg/ml brefeldin A prior to intracellular IFN-γ staining. As a positive control, hepatocytes, LSEC, Kupffer cells or DCs were pulsed 1 hr with Cor93 or Env28 peptides and washed three times to remove excess peptide prior to incubation with CD8 T_E.

Immunofluorescence Staining and Histochemistry

Livers were perfused with PBS, harvested and fixed in 4% paraformaldehyde for 16 hr, then dehydrated in 30% sucrose prior to embedding in OCT freezing media (Bio-Optica). Thirty micrometer sections were cut on a CM1520 cryostat (Leica) and adhered to Superfrost Plus slides (Thermo Scientific). Sections were then permeabilized and blocked in PBS containing 0.3% Triton X-100 (Sigma-Aldrich) and 10% FBS followed by staining in the same blocking buffer. The following primary Abs were used for staining: anti-VCAM-1 (429[MVCAM.A], BioLegend), anti ICAM-1 (NY1/1.7.4, BioLegend), anti-PECAM-1 (MEC13.3, BioLegend), anti-CD62E (10E9.6, BD), anti-CD62P (RB40.34, BD), anti-collagen IV (polyclonal, Abcam), anti-Lyve-1 (polyclonal, Novus Biologicals), anti-CD41 (MWReg30, BioLegend), anti-HBcAg (polyclonal, Dako), Alexa Fluor 647-conjugated anti-IFN-γ (XMG1.2, BioLegend), anti-active caspase 3 (polyclonal, R&D). In some experiments anti-HBcAg, anti-Lyve-1 an anti-collagen IV were directly conjugated using the Zenon Alexa Fluor 568 or 647 rabbit IgG labeling kit (Life Technologies). The following secondary Abs were used for staining: Alexa Fluor 488-, 514-, 568- or 647-conjugated goat anti-rabbit IgG (Life Technologies), Alexa Fluor 647-conjugated chicken anti-rat IgG. Stained slides were mounted with Fluorsave (Merck Millipore) and images were acquired on an inverted Leica microscope (TCS

STED CW SP5, Leica Microsystems) with a motorized stage for tiled imaging. To minimize fluorophore spectral spillover, we used the Leica sequential laser excitation and detection modality. The bleed-through among sequential fluorophore emission was removed applying simple compensation correction algorithms to the acquired images. The semiautomatic surface-rendering module in Imaris (Bitplane) was used to create 3D volumetric surface objects corresponding either to individual cells or to the liver vascular system. Signal thresholds were determined using the Imaris Surface Creation module, which provides automatic threshold identification and value-based visual surface thresholding around the positively stained objects.

For the semiquantitative analysis of platelet adhesion to liver sinusoids (Figure S2C), high resolution confocal xyz stacks of 30 xy sections (1024 × 1024 pixel) sampled with 1 μm z spacing were acquired to provide image volumes of 388 × 388 × 30 μm^3. The confocal z stacks were imported into Imaris software (Bitplane) and platelets were reconstructed as 3D volumes by means of the semiautomatic surface-rendering module with a seed point diameter of 2.08 μm (the mean platelet diameter) (Thon et al., 2012). The split touching objects option of the module supports the separation of two or more objects that are identified as one, enabling the splitting of aggregates into single components.

For the quantification of cells inside liver sinusoids, confocal xyz stacks of 30-60 square xy sections (1024 × 1024 pixel) sampled with 1 μm z-spacing were acquired to provide image volumes 30-60 μm in depth and with an xy field of view variable between 100 × 100 μm^2 and 388 × 388 μm^2. The Imaris Surpass View and Surface Creation Wizard were used to create 3D renderings of both cells and liver sinusoids. A cell was considered intravascular if at least 95% of its surface-reconstructed body was inside the vessel lumen in all the acquired sections projected in the horizontal (xy), transversal (yz) and longitudinal (xz) planes. This analysis was performed both by visual inspection of the xyz projections within the Imaris Section View Menu and by tracing the fluorescence intensity profiles of the channels related to cells and sinusoids walls. Only cells completely contained within the xyz stacks were considered for the analysis and out of focus cells were discarded.

For H&E, Sirius red and HBcAg stainings, livers were perfused with PBS, harvested in Zn-formalin and transferred into 70% ethanol 24 hr later. Tissue was then processed, embedded in paraffin and stained as previously described (Sitia et al., 2011, 2012). Bright-field images were acquired through an Aperio Scanscope System CS2 microscope and an ImageScope program (Leica Biosystem) following the manufacturer's instructions. Quantification of Sirius Red^+ area was performed as described (Sitia et al., 2012).

Intravital Epifluorescence Microscopy

A tail vein catheter (VisualSonic) was inserted into previously shaved mice prior to anesthetization with 5% isoflurane (Abbot) through a nose cone also delivering oxygen at 1L/min. Follow-up surgery and liver intravital imaging were carried out with lower concentrations of isoflurane (between 0.8% and 1%). Surgical preparation of the liver was performed as described (Sitia et al., 2011). An upright Axiotech Vario microscope (Carl Zeiss) - enclosed in an environmental chamber capable of maintaining a temperature of 37-38°C and equipped with a Colibri system of high-performance Light Emitting Diodes - was used for intravital visualization. Continuous body temperature monitoring through a rectal probe was performed to ensure that a narrow range of 37–38°C was maintained at all times. Images were acquired with an Orca-D2 camera (Hamamatsu) at an acquisition rate of 10-30 frames/second. 2D positions of cell centroids were segmented by semi-automated cell tracking algorithms of Imaris (Bitplane). To quantify the sticking fraction and the number of circulating cells, cell tracks, and displacement between consecutive time points were calculated using custom designed scripts in Matlab (MathWorks). The sticking fraction was defined as the percentage of total cells that became firmly adherent to liver sinusoids for > 30 s. Circulating cells were defined as the total number of cells that entered the field of view during the observation period (1 min for Figure 1B and 10 min for Figure 3C). The results were further confirmed by visual inspection of the acquired videos.

Intravital Multiphoton Microscopy

Tail vein catheterization and anesthetic procedures were carried out as above. After opening the skin with a midline incision and detaching peritoneal adherences, midline and left subcostal incisions were made in the peritoneum through a high-temperature cautery. The falciform ligament was resected and mice were placed in a left lateral position with the left liver lobe gently exteriorized onto a glass coverslip attached to a custom-made imaging platform. The liver was covered with plastic wrap, the incision was packed with moist gauze, and the imaging platform was sealed to prevent dehydration. Liver sinusoids were visualized by injecting nontargeted Quantum Dots 655 (Invitrogen) i.v. immediately prior to imaging. Images were acquired with a LaVision BioTec TriMScope II coupled to a Nikon Ti-U inverted microscope enclosed in a custom-built environmental chamber (Life Imaging Services) that was maintained at 37-38°C with heated air. Continuous body temperature monitoring through a rectal probe was performed to ensure that a narrow range of 37–38°C was maintained at all times. Fluorescence excitation was provided by two tunable fs-pulsed Ti:Sa lasers (680–1080 nm, Ultra II, Coherent). The setup includes four photomultiplier tubes (3 Hamamatsu H7422-40 GaAsP High Sensitivity PMTs and 1 Hamamatsu H7422-50 GaAsP High Sensitivity red-extended PMT) and a high working distance water-immersion 20x objective (NA = 1.0, Zeiss). For 4D analysis of cell migration, stacks of 7-9 square xy sections (512 × 512 pixel) sampled with 4 μm z spacing were acquired every 5-10 s for up to 2 hr to provide image volumes that were 40 μm in depth and with an xy field of view variable between 100 × 100 μm^2 and 450 × 450 μm^2. Sequences of image stacks were transformed into volume-rendered, 4D time-lapse movies with Imaris (Bitplane). The 3D positions of the cell centroids were segmented by semi-automated cell tracking algorithm of Imaris. The mean 3D velocity, the displacement (distance between the initial and the final position of a cell) and the confinement ratio (displacement over distance) were calculated from the x, y, and z coordinates of the cell centroids using custom

designed scripts in Matlab (MathWorks). CD8 T_E were defined as adjacent to hepatocytes when they lied within a radius of 15 μm around the hepatocyte centroid.

Transmission and Scanning Electron Microscopy

After PBS perfusion, livers were fixed in situ by portal vein injection of 1.5% glutaraldehyde 2% paraformaldehyde in 0.1 M sodium cacodylate buffer (pH 7.4). Livers were excised and immersed in the same solution for 16h. For transmission electron microscopy (TEM) analyses, samples were processed as described (Junt et al., 2007) and imaged with a ZEISS Leo912AB Omega fitted with a 2k × 2k bottom-mounted slow-scan Proscan camera controlled by the EsivisionPro 3.2 software. For scanning electron microscopy (SEM) analyses, samples were processed as described (Warren et al., 2006) and examined under a ZEISS SIGMA scanning electron microscope.

Morphometric Quantitation of Sinusoidal Fenestrae

Porosity, the percentage of liver endothelial surface area occupied by fenestrae, was calculated from SEM images from 3 control and 3 arsenite-treated mice using ImageJ software (National Institute of Health). Hepatic zones were identified based on extracellular matrix deposition around the large vessels and visualization of bile ducts, as described (Straub et al., 2007). Representative images from each of the three identified hepatic zones in at least 5 sinusoids per mouse were acquired and a total area of ~3000 μm^2 was analyzed for each mouse. The image brightness and contrast were adjusted for sharp definition of the edges of each fenestra. A threshold was then applied to the images, and the area occupied by fenestrae relative to the total sinusoid area was quantified with the ImageJ Analyze Particle function.

Correlative Confocal and Transmission Electron Microscopy and Tomography

Livers from Alb-cre x $ROSA^{mT/mG}$ x HBcAg transgenic mice that were transferred 30 min earlier with 4 × 10^7 Bodipy-labeled Cor93 CD8 T_E were perfused with PBS and fixed in situ by portal vein injection of 1.5% glutaraldehyde 2% paraformaldehyde in 0.1 M sodium cacodylate buffer (pH 7.4). Livers were excised and immersed in the same solution for 16h. Fixed samples were dehydrated in 2.5 M sucrose prior to embedding in OCT and 30 μm sections were cut and processed for confocal imaging using PBS as mounting medium to prevent dehydration. After confocal image acquisition, the coverslips were gently removed and sections adherent to the slide were processed for TEM as described (Junt et al., 2007). The BEEM capsules containing the embedded sections were detached by immerging the slides in liquid nitrogen, leaving the section facing up on the resin block. The specimens were mounted on a Leica Ultracut UCT and 200-250 nm thick sections were collected on formvar-coated copper slot grids. The Z position as well as the blood vessel morphology were used to acquire electron micrographs corresponding to the same field of view acquired by confocal imaging. Images were then rotated to match cell contours, and overlay of aligned images yielded optical–electron microscopy correlations.

For electron tomography, 15 nm-gold fiducials were applied on both surfaces of the grids. The samples were imaged on a 200 kV Tecnai G2 20 electron microscope (FEI, Eindhoven) at a magnification of 2.5K or 11.5K, resulting in pixel sizes of 8.99 nm and 1.95 nm, respectively. Single- or double-tilted image series (±60°/65° according to a Saxton scheme with the initial tilt step of 7° for the low and 2° for the higher magnification) were acquired using Xplorer 3D (FEI, Eindhoven) with an Eagle 2,048 × 2,048 CCD camera (FEI, Eindhoven). Tilted series alignment and tomographic reconstructions were done with the IMOD software package (Kremer et al., 1996). The semiautomatic surface-rendering module in Imaris (Bitplane) was used to create 3D volumetric surface objects corresponding either to CD8 T_E or LSEC.

DNA and RNA Analyses

Total DNA and RNA were isolated from frozen livers (left lobe) for analyses by Southern blot, RNase protection (RPA) and real-time PCR as previously described (Iannacone et al., 2008). Nylon membranes were analyzed for HBV DNA as previously described (Iannacone et al., 2005). Analysis of chemokine mRNAs was performed by RPA as previously described (Kakimi et al., 2001). For qRT-PCR, 1 μg of total hepatic RNA was reverse transcribed prior to qPCR analysis for HBsAg (Thimme et al., 2003) and IFN-γ with TaqMan probes (Applied Biosystems). All experiments were done in triplicate and normalized to the housekeeping gene GAPDH.

Biochemical Analyses

The extent of hepatocellular injury was monitored by measuring sALT activity at multiple time points after treatment as previously described (Sitia et al., 2012).

Statistical Analyses

Results are expressed as mean ± SEM. All statistical analyses were performed in Prism 5 (GraphPad Software). Means between two groups were compared with two-tailed t test. Means among three or more groups were compared with one-way or two-way ANOVA with Bonferroni post-test.

SUPPLEMENTAL REFERENCES

Junt, T., Moseman, E.A., Iannacone, M., Massberg, S., Lang, P.A., Boes, M., Fink, K., Henrickson, S.E., Shayakhmetov, D.M., Di Paolo, N.C., et al. (2007). Subcapsular sinus macrophages in lymph nodes clear lymph-borne viruses and present them to antiviral B cells. Nature *450*, 110–114.

Kakimi, K., Lane, T.E., Wieland, S., Asensio, V.C., Campbell, I.L., Chisari, F.V., and Guidotti, L.G. (2001). Blocking chemokine responsive to gamma-2/interferon (IFN)-gamma inducible protein and monokine induced by IFN-gamma activity in vivo reduces the pathogenetic but not the antiviral potential of hepatitis B virus-specific cytotoxic T lymphocytes. J. Exp. Med. *194*, 1755–1766.

Kramer, M.G., Barajas, M., Razquin, N., Berraondo, P., Rodrigo, M., Wu, C., Qian, C., Fortes, P., and Prieto, J. (2003). In vitro and in vivo comparative study of chimeric liver-specific promoters. Mol. Ther. *7*, 375–385.

Kremer, J.R., Mastronarde, D.N., and McIntosh, J.R. (1996). Computer visualization of three-dimensional image data using IMOD. J. Struct. Biol. *116*, 71–76.

Sitia, G., Aiolfi, R., Di Lucia, P., Mainetti, M., Fiocchi, A., Mingozzi, F., Esposito, A., Ruggeri, Z.M., Chisari, F.V., Iannacone, M., and Guidotti, L.G. (2012). Antiplatelet therapy prevents hepatocellular carcinoma and improves survival in a mouse model of chronic hepatitis B. Proc. Natl. Acad. Sci. USA *109*, E2165–E2172.

Smedsrød, B., and Pertoft, H. (1985). Preparation of pure hepatocytes and reticuloendothelial cells in high yield from a single rat liver by means of Percoll centrifugation and selective adherence. J. Leukoc. Biol. *38*, 213–230.

Thimme, R., Wieland, S., Steiger, C., Ghrayeb, J., Reimann, K.A., Purcell, R.H., and Chisari, F.V. (2003). CD8(+) T cells mediate viral clearance and disease pathogenesis during acute hepatitis B virus infection. J. Virol. *77*, 68–76.

Thon, J.N., Macleod, H., Begonja, A.J., Zhu, J., Lee, K.-C., Mogilner, A., Hartwig, J.H., and Italiano, J.E., Jr. (2012). Microtubule and cortical forces determine platelet size during vascular platelet production. Nat. Commun. *3*, 852.

Vanrell, L., Di Scala, M., Blanco, L., Otano, I., Gil-Farina, I., Baldim, V., Paneda, A., Berraondo, P., Beattie, S.G., Chtarto, A., et al. (2011). Development of a liver-specific Tet-on inducible system for AAV vectors and its application in the treatment of liver cancer. Mol. Ther. *19*, 1245–1253.

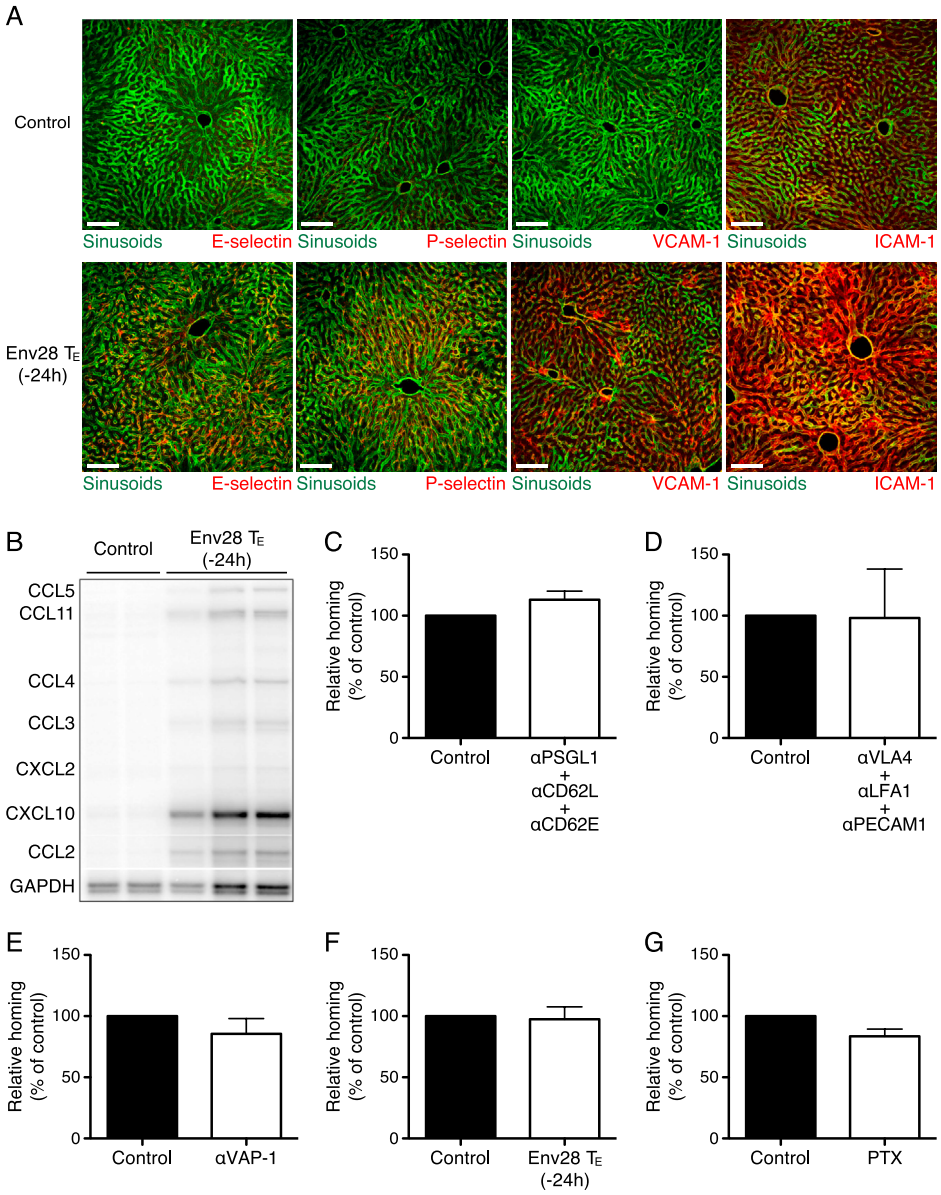

Figure S1. Hepatic Accumulation of CD8 T_E Is Independent of Selectins, β2- and α4-Integrins, PECAM-1, Vascular Adhesion Protein (VAP)-1, and Gαi-Coupled Receptor Signaling Capability, Related to Figure 2

(A) Representative liver confocal micrographs from HBV replication-competent transgenic mice either prior to (control) or 24 hr after Env28 CD8 T_E injection showing E-selectin, P-selectin, VCAM-1 or ICAM-1 expression in liver sinusoids. Scale bars represent 50 μm.

(B) Total hepatic RNA from the same mice described in (A) was analyzed for the expression of the indicated chemokines by RNase protection assay. The image represents a single gel, from which irrelevant lines were spliced out, as represented by the marked lines.

(C) Percentage of GP33 CD8 T_E (in vivo generation of GP33-specific CD8 T_E is described in Experimental Procedures) that accumulated within the liver 2 hr upon transfer into C57BL/6 mice that were previously treated with anti-PSGL1, anti-CD62L and anti-CD62E Abs relative to control (control = 100%). n = 4; results are representative of 2 independent experiments.

(D) Percentage of GP33 CD8 T_E that accumulated within the liver 2 hr upon transfer into C57BL/6 mice that were previously treated with anti-VLA-4, anti-LFA-1 and anti-PECAM-1 Abs relative to control (control = 100%). n = 4; results are representative of 2 independent experiments.

(E) Percentage of GP33 CD8 T_E that accumulated within the liver 2h upon transfer into C57BL/6 mice that were previously treated with anti-VAP-1 Abs relative to control (control = 100%). n = 4; results are representative of 2 independent experiments.

(F) Percentage of GP33 CD8 T_E that accumulated within the liver 2 hr upon transfer into HBV replication-competent transgenic mice ($H2^{bxd}$) that were treated 24 hr earlier with 5×10^6 Env28 CD8 T_E (which caused endothelial activation as shown in (A) relative to control. n = 5; results are representative of 2 independent experiments.

(G) Percentage of PTX-treated GP33 CD8 T_E that accumulated within the liver 2 hr upon transfer into C57BL/6 mice relative to control GP33 CD8 T_E. n = 5; results are representative of 2 independent experiments.

Results are expressed as mean ± SEM.

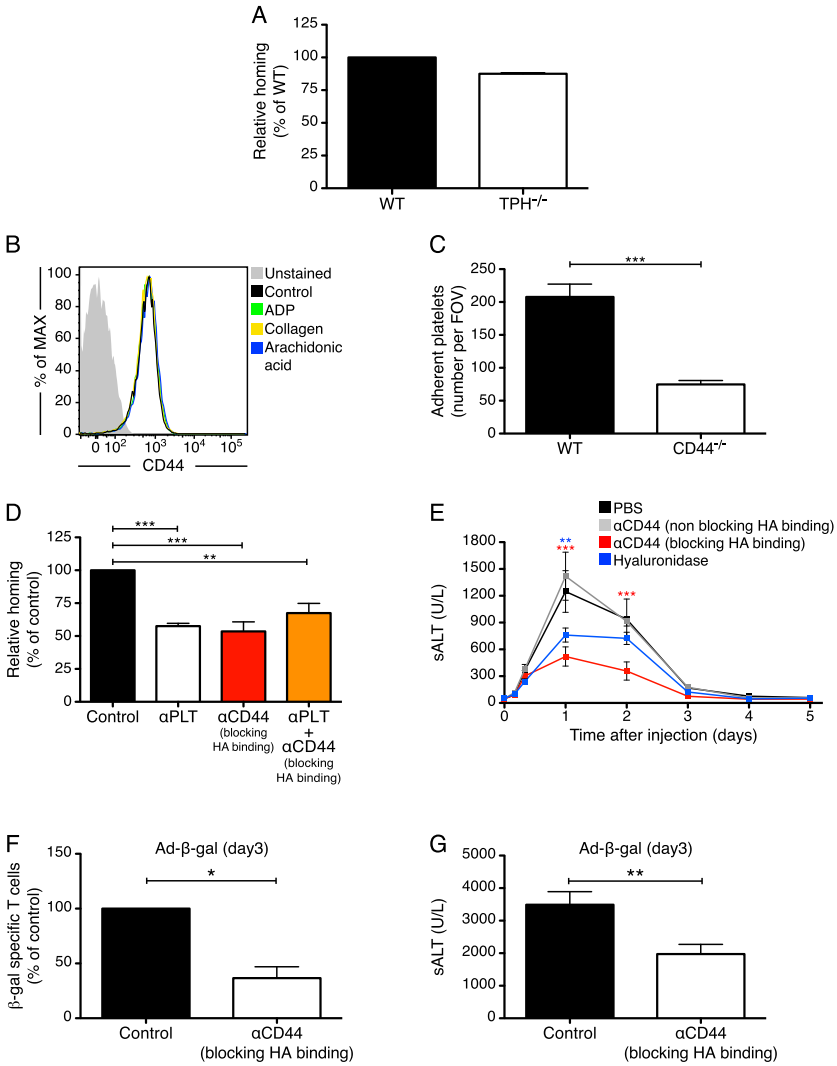

Figure S2. Hepatic CD8 T_E Accumulation Requires Platelets that Have Adhered to Sinusoidal Hyaluronan via CD44, Related to Figure 3

(A) Percentage of Cor93 CD8 T_E recovered 2 hr after injection from the livers of serotonin-deficient HBV replication-competent transgenic mice ($TPH^{-/-}$) relative to serotonin-competent HBV replication-competent transgenic mice (WT = 100%). n = 4; results are representative of 2 independent experiments. Note that the use of serotonin-deficient mice (instead of reconstitution experiments with serotonin-deficient platelets) is dictated by the fact that platelets from $TPH^{-/-}$ mice take up serotonin secreted from enterochromaffin cells in the gastrointestinal tract of WT recipient mice (data not shown).

(B) FACS plots showing the expression of CD44 on WT platelets that were either left untreated (control) or stimulated with the platelet agonist ADP, collagen or arachidonic acid. Plots are representative of 2 independent experiments.

(C) Quantification of the number of adherent platelets per field of view (FOV) in C57BL/6 (WT) or $CD44^{-/-}$ livers. 9 fields of view in 3 different mice per group were analyzed.

(D) Percentage of Cor93 CD8 T_E that accumulated within the liver 2 hr upon transfer into HBV replication-competent x mGP-Ibα^{null};hGP-Ibα^{Tg} mice that were previously depleted of platelets (αPLT, white), treated with anti-CD44 Abs (clone KM81 that blocks CD44 binding to hyaluronan [HA], red) or both (orange), relative to control (control = 100%). n = 7; results are representative of 2 independent experiments.

(E) ALT activity, measured at the indicated time points after the injection of Cor93 CD8 T_E, in the serum of HBV replication-competent transgenic mice ($H2^{bxd}$) that were previously treated with PBS (black), anti-CD44 (clone IM7 that does not block CD44 binding to hyaluronan [HA]) Abs (gray), anti-CD44 (clone KM81 that blocks CD44 binding to hyaluronan [HA]) Abs (red) or hyaluronidase (blue). n = 4; results are representative of 3 independent experiments.

(F and G) Three weeks after DNA immunization with a β-gal-expressing plasmid, C57BL/6 mice were bled, grouped based on the relative frequency of circulating β-gal-specific CD8 T_E (~2% of the total circulating CD8+ T cells, data not shown) and injected with 3×10^9 pfu of an hepatotropic adenovirus encoding for β-gal (Ad-β-gal). One day after Ad-β-gal-injection (a time point by which Ad-β-gal has reached its peak hepatocellular expression, data not shown), mice were treated or not with anti-CD44 Abs (clone KM81 that blocks CD44 binding to hyaluronan [HA]) and, two days later, sacrificed for analyses of the absolute number of hepatic β-gal-specific CD8 T_E (F) and the relative serum ALT levels (G). n = 4; results are representative of 2 independent experiments.

Results are expressed as mean ± SEM. *p < 0.05, **p < 0.01, ***p < 0.001.

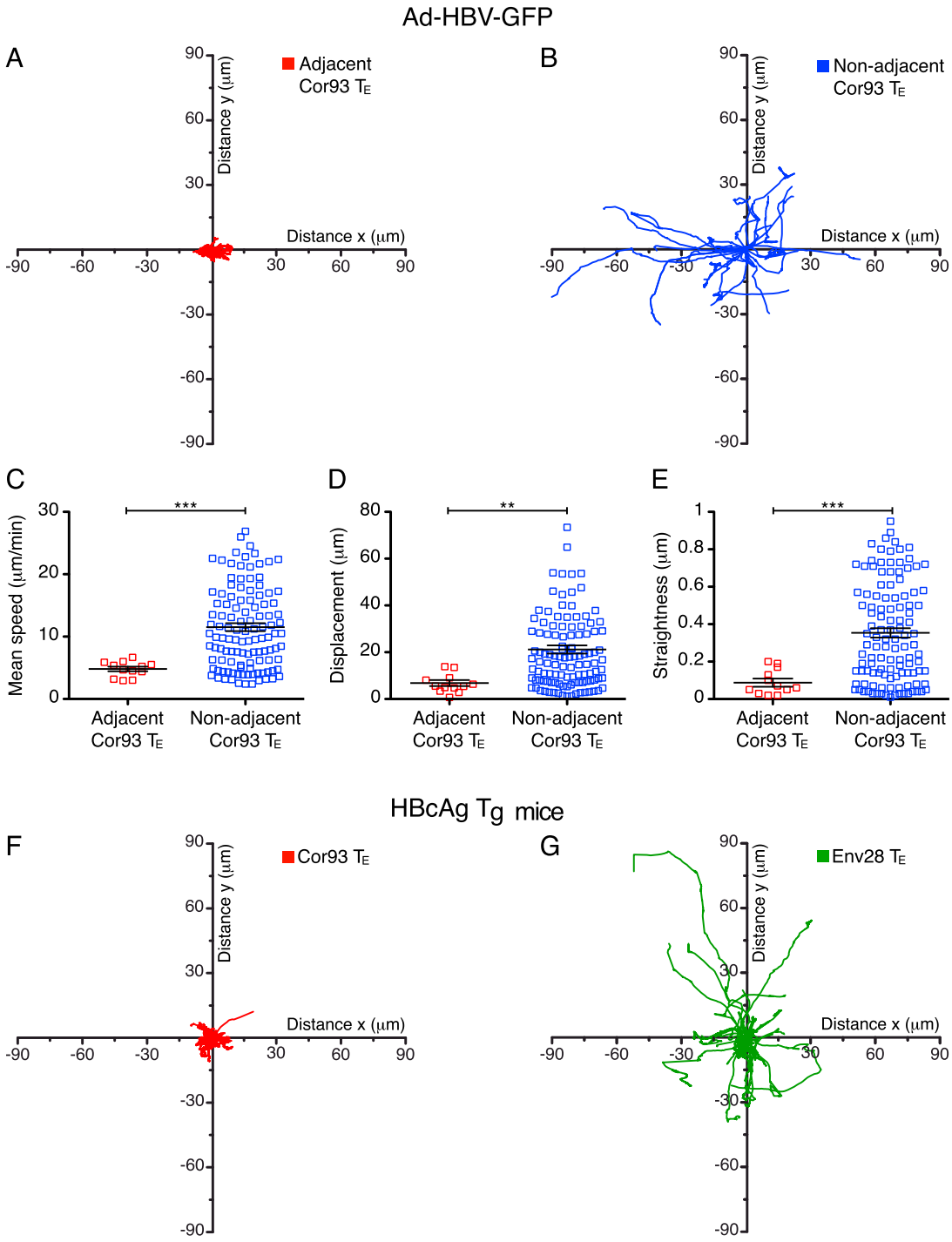

Figure S3. CD8 T_E Crawl along Liver Sinusoids until Hepatocellular Ags Are Recognized, Related to Figure 4

(A and B) C57BL/6 mice were injected with Ad-HBV-GFP two days prior to Cor93 CD8 T_E transfer. Track plots of Cor93 CD8 T_E that are adjacent (A) or not (B) to Ag-expressing hepatocytes were recorded during a 30 min observation period. Each track has been shifted such that it starts at the origin of the x and y axes. Results are representative of 2 independent experiments. See also Movie S4.

(C–E) Mean speed (C), displacement (D) and straightness (E) of individual Cor93 CD8 T_E that were adjacent or not to Ag-expressing hepatocytes in the liver of C57BL/6 mice that were injected with Ad-HBV-GFP two days prior to Cor93 CD8 T_E transfer. Data are representative of 2 independent experiments.

(F and G) Track plots of Cor93 CD8 T_E (F) and Env28 CD8 T_E (G) in the liver of a HBcAg transgenic mouse ($H2^b$) during a 30 min observation period. Each track has been shifted such that it starts at the origin of the x and y axes. Results are representative of 3 independent experiments. See also Movie S5.

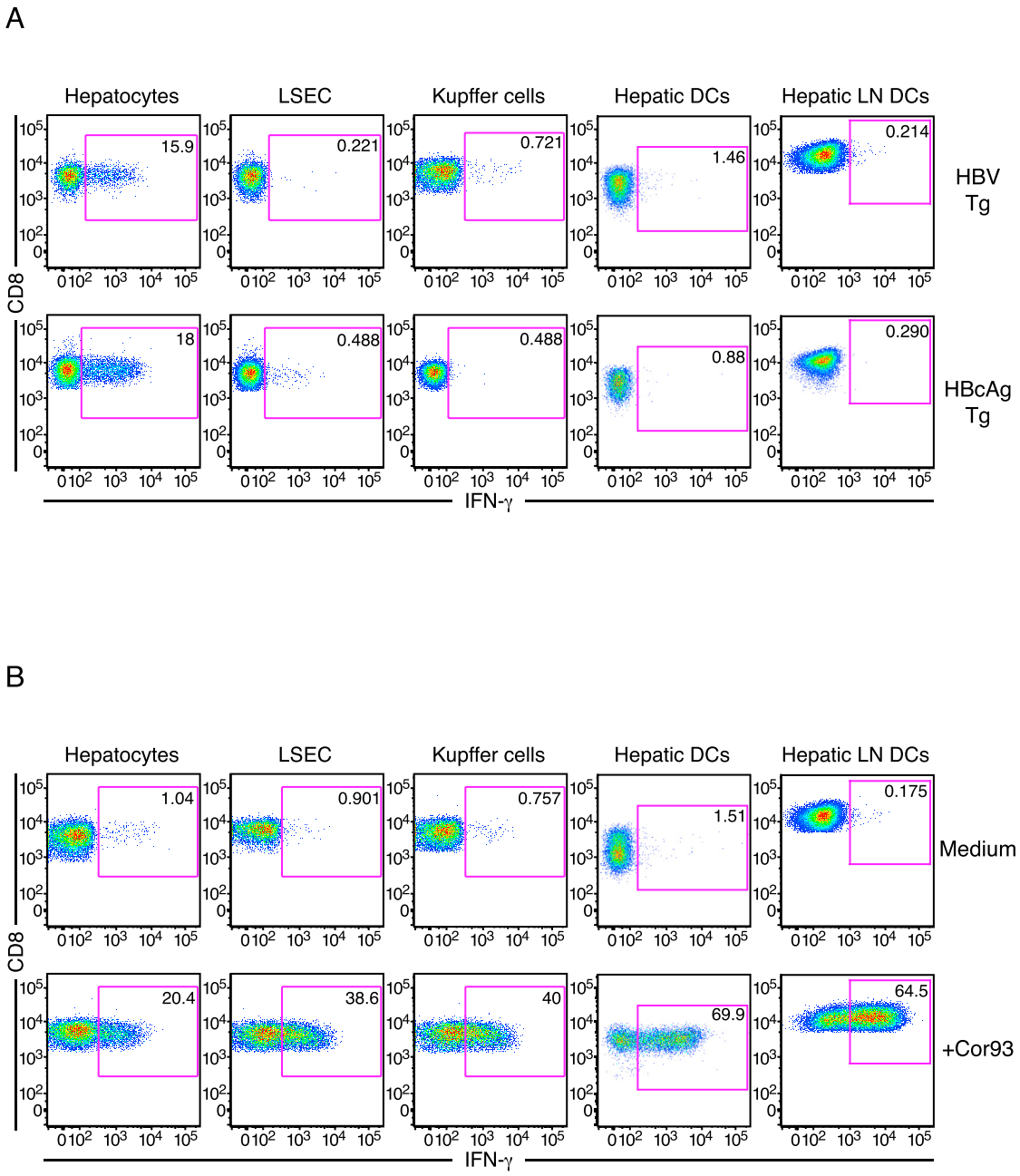

Figure S4. HBcAg Presentation to CD8 T_E in HBV Replication-Competent and HBcAg Transgenic Mice Is Restricted to Hepatocytes, Related to Figure 4

(A) Hepatocytes, LSEC, Kupffer cells, hepatic dendritic cells (DCs) or hepatic lymph node (LN) DCs isolated from HBV replication-competent transgenic $H2^b$ mice (top) or HBcAg transgenic $H2^b$ mice (bottom) were incubated with Cor93 CD8 T_E (see Experimental Procedures). Five hours later cells were assessed for their capacity to produce IFN-γ by flow cytometry. Results are representative of 3 independent experiments.

(B) To control for sensitivity, specificity, and peptide-presentation capacity of the results shown in (A), hepatocytes, LSEC, Kupffer cells, hepatic DCs or hepatic LN DCs isolated from control C57BL/6 mice were pulsed with Cor93 peptide (bottom) or not (top) prior to incubating them with Cor93 CD8 T_E (see Experimental Procedures). Five hours later, cells were assessed for their capacity to produce IFN-γ by flow cytometry. Results are representative of 3 independent experiments. Similar results were obtained when hepatocytes, LSEC, Kupffer cells, hepatic DCs or hepatic LN DCs isolated from HBV replication-competent transgenic $H2^d$ mice were incubated with Env28 CD8 T_E (data not shown).

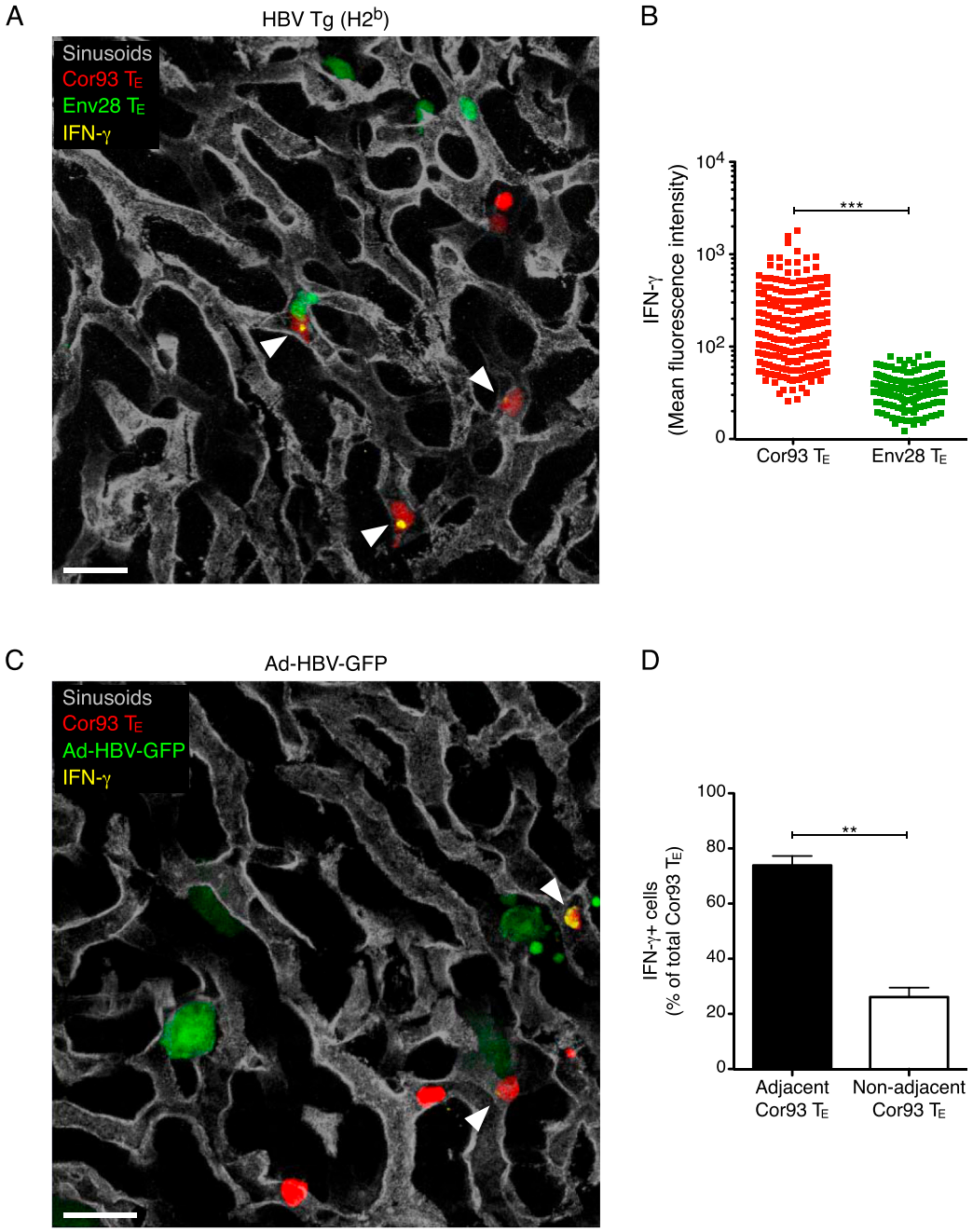

Figure S5. Quantification of IFN-γ Stainings, Related to Figure 5

(A) Representative confocal micrographs of the liver of a HBV replication-competent transgenic mouse ($H2^b$) that was injected 2 hr earlier with Cor93 (red) and Env28 (green) CD8 T_E. Sinusoids are shown in gray and IFN-γ in yellow. Scale bar represents 20 μm. See also Movie S6. Similar results were obtained in similarly treated HBcAg transgenic mice (data not shown).

(B) IFN-γ mean fluorescent intensity of Cor93 (red, n = 209) and Env28 (green, n = 182) CD8 T_E measured in the same mice described in (A).

(C) Representative confocal micrographs of the liver of a C57BL/6 mouse that was injected with Ad-HBV-GFP two days prior to Cor93 (red) CD8 T_E transfer. Sinusoids are shown in gray, IFN-γ in yellow and GFP signal in green. Scale bar represents 10 μm.

(D) Quantification of the number of IFN-γ^+ Cor93 CD8 T_E that were adjacent or not to Ag-expressing hepatocytes in the same mice described in (C). n = 388 cells. Results are expressed as mean ± SEM. $^{**}p < 0.01$, $^{***}p < 0.001$.

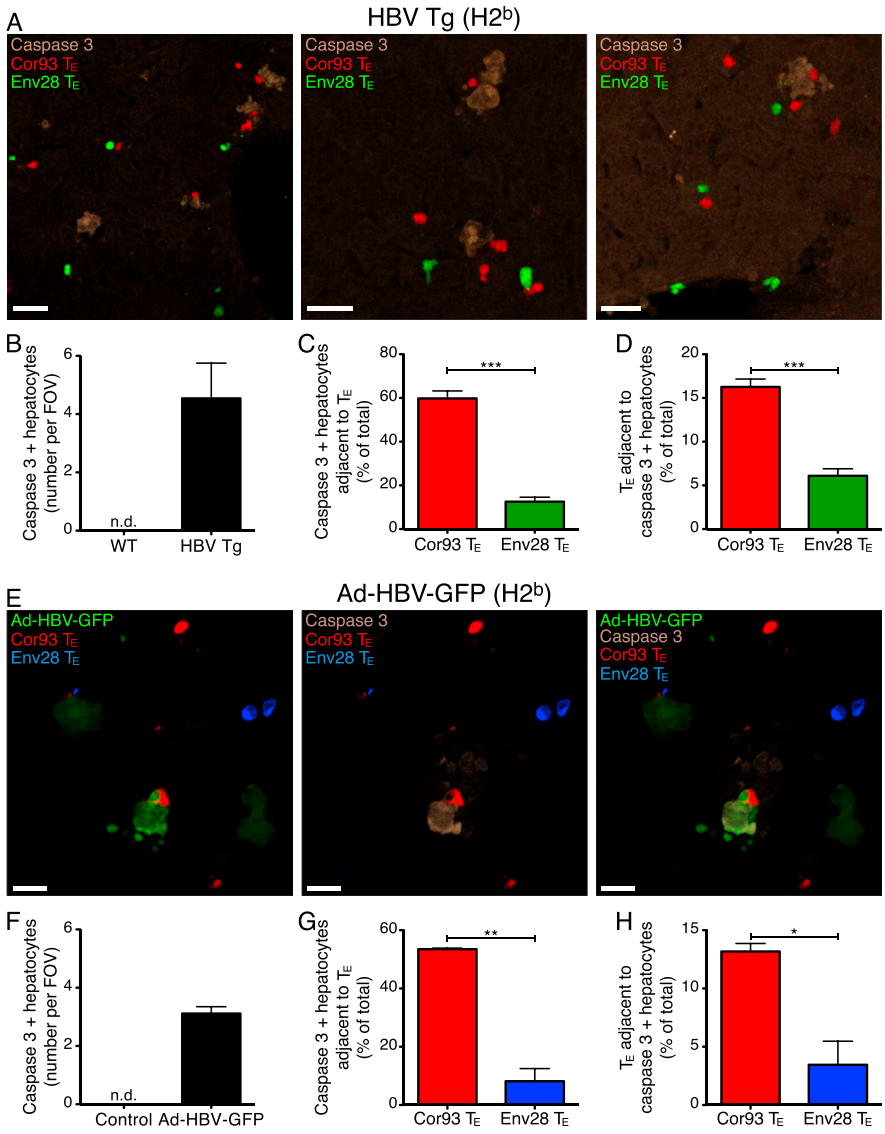

Figure S6. Localization of Ag-Specific and Non Ag-Specific CD8 T_E Relative to Apoptotic Hepatocytes, Related to Figure 5

(A) Representative confocal micrographs of the liver of HBV replication-competent transgenic mice ($H2^b$) that were injected 2 hr earlier with Cor93 CD8 T_E (red) and Env28 CD8 T_E (green). Caspase 3 signal is shown in brown. Scale bars represent 30 μm.

(B) Quantification of the number of caspase 3^+ hepatocytes per field of view (FOV) in the liver of HBV replication-competent transgenic or wild-type mice (both $H2^b$) that were injected 2 hr earlier with Cor93 (red) and Env28 (green) CD8 T_E. n = 19 (HBV Tg) and 18 (WT) FOV.

(C) Quantification, in the same mice described in (A), of the percentage of caspase 3^+ hepatocytes that had at least 1 adjacent Cor93 (red) or Env28 (green) CD8 T_E. n = 85 caspase 3^+ hepatocytes.

(D) Quantification, in the same mice described in (A), of the percentage of Cor93 (red) or Env28 (green) CD8 T_E that were adjacent to caspase 3^+ hepatocytes. n = 376 (Cor93 T_E) and 183 (Env28 T_E).

(E) Representative liver confocal micrographs from a C57BL/6 mouse that was injected with Ad-HBV-GFP 2 days prior to Cor93 (red) and Env28 (blue) CD8 T_E transfer. GFP signal is shown in green (left and right panels) and caspase 3 signal in brown (middle and right panels). Scale bars represent 15 μm.

(F) Quantification of the number of caspase 3^+ hepatocytes per field of view (FOV) in the liver of wild-type mice ($H2^b$) that were injected or not with Ad-HBV-GFP prior to Cor93 and Env28 CD8 T_E transfer. n = 18 FOV.

(G) Quantification, in the same mice described in (E), of the percentage of caspase 3^+ hepatocytes that had at least 1 adjacent Cor93 (red) or Env28 (blue) CD8 T_E. n = 58 caspase 3^+ hepatocytes.

(H) Quantification, in the same mice described in (E), of the percentage of Cor93 (red) or Env28 (blue) CD8 T_E that were adjacent to caspase 3^+ hepatocytes. n = 237 (Cor93 T_E) and 143 (Env28 T_E).

Results are expressed as mean ± SEM. *p < 0.05, **p < 0.01, ***p < 0.001.

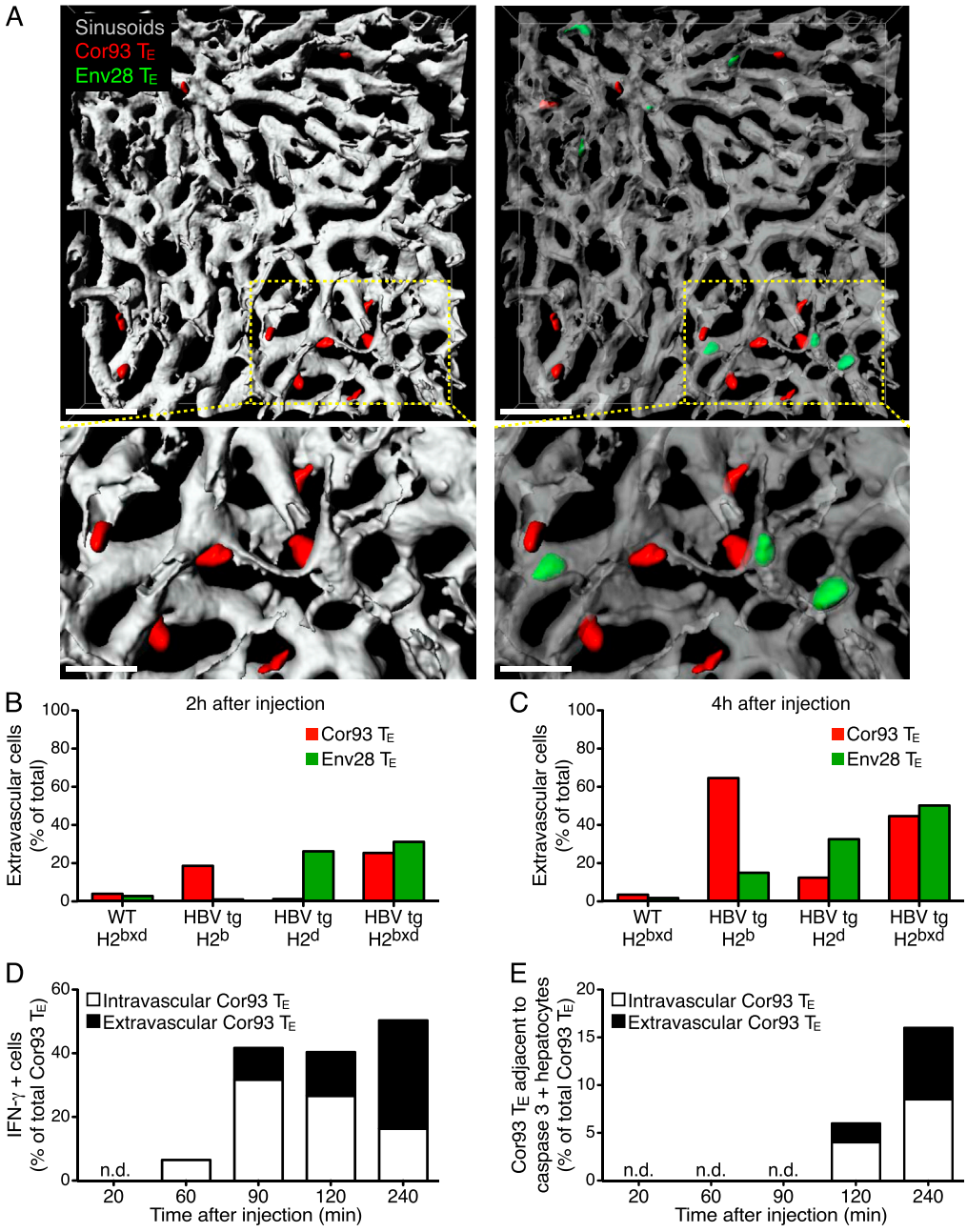

Figure S7. Hepatocellular Ag Recognition Is Required for CD8 T_E Extravasation, Related to Figure 5

(A) Representative confocal micrographs of the liver of a HBV replication-competent transgenic mouse ($H2^b$) that was injected 4 hr earlier with Cor93 (red) and Env28 (green) CD8 T_E. To allow visualization of intravascular events and to enhance image clarity, the transparency of the sinusoidal rendering in the right panels was set to 60%. Scale bars represent 40 μm (upper panels) and 10 μm (lower panels).

(B and C) The percentage of extravascular Cor93 (red) and Env28 (green) CD8 T_E in the livers of WT or HBV replication-competent transgenic mice ($H2^b$, $H2^d$ or $H2^{bxd}$) was assessed 2 hr (B) or 4 hr (C) after CD8 T_E transfer. Data were obtained by assessing at least 200 Cor93 CD8 T_E and 200 Env28 CD8 T_E in 2 mice per strain. Results are representative of 2 independent experiments.

(D) The percentage of intravascular (white) and extravascular (black) IFN-γ^+ Cor93 CD8 T_E in the livers of HBV replication-competent transgenic mice ($H2^{bxd}$) was assessed at the indicated time points after CD8 T_E transfer. n = 150 (60 min), 162 (90 min), 614 (120 min), 748 (240 min).

(E) The percentage of intravascular (white) and extravascular (black) Cor93 CD8 T_E that were adjacent to apoptotic hepatocytes in the livers of HBV replication-competent transgenic mice ($H2^{bxd}$) was assessed at the indicated time points after CD8 T_E transfer. n = 21 (120 min), 98 (240 min).